Journal of Applied Polymer Science

Plasma treatment of wood-polymer composites: A comparison of three different discharge types and their effect on surface properties

Benedikt Hünnekens,[1] Frauke Peters,[2] Georg Avramidis,[2,3] Andreas Krause,[4] Holger Militz,[1] Wolfgang Viöl[2,3]

[1]Wood Biology and Wood Products, Burckhardt-Institute, Georg August University of Göttingen, Büsgenweg 4, Göttingen 37077, Germany

[2]Faculty of Natural Sciences and Technology, University of Applied Sciences and Arts, Von-Ossietzky-Str. 99, Göttingen 37085, Germany

[3]Fraunhofer Application Centre for Plasma and Photonic, Von-Ossietzky-Straße 100, Göttingen 37085, Germany

[4]Mechanical Wood Technology, University of Hamburg, Leuschnerstraße 91C, Hamburg 21031, Germany

Correspondence to: B. Hünnekens (E-mail: bhuenne@gwdg.de)

ABSTRACT: Three different discharge types, based on the principle of a dielectric barrier discharge at atmospheric pressure, were investigated with regard to their influence on the adhesion properties of a series of wood–polymer composites. Wood flour (*Picea abies L.*) filled polypropylene and various proportions of polyethylene were manufactured either through extrusion or injection molding. The composites' surfaces were activated by coplanar surface barrier discharge, remote plasma, and direct dielectric barrier discharge. The changes in wettability due to the pretreatment were investigated by contact angle measurement using the sessile drop method and calculation of surface free energy (SFE). It could be shown that wettability was improved by all three types of discharge, the contact angle decreased and the SFE correspondingly increased. X-ray photoelectron spectroscopy revealed an increase in the *O*/*C* ratio at the material's surface. An improvement in coating adhesion was demonstrated by crosscut and pulloff tests. © 2016 Wiley Periodicals, Inc. J. Appl. Polym. Sci. **2016**, *133*, 43376.

KEYWORDS: cellulose and other wood products; coatings; composites; surfaces and interfaces; thermoplastics

Received 30 September 2015; accepted 22 December 2015

DOI: 10.1002/app.43376

INTRODUCTION

The application fields of wood–polymer composites (WPC) are diverse. These materials are widely used in many sectors, including the building and construction industry, the automotive industry or the furniture industry, for which they provide products, such as claddings, fencing, and window frames.[1,2]

The greatest volume, however, is generated by the production of deckings made of the two main matrix polymers polypropylene (PP) and polyethylene (PE) for exterior application in the North American and European markets. Other fast growing markets include China and Japan.[3]

Durability is one of the most important required properties of the composites in outdoor application. But due to weathering processes, the material is physically influenced and degraded by UV radiation, moisture, temperature, and air pollutants.[4,5] As Stark and Matuana[6] and Ndiaye *et al.*[7] confirm, these degradation processes affect both, the polymer matrix and the wood and its components—cellulose, hemicelluloses, lignin, and extractives.[8,9] To achieve an appropriate outdoor performance, protective coatings and paints can be applied to the composites' surface.[10]

Taking into account that the surface properties of WPC are mainly influenced by the polymers PP and PE which are of low polarity, problems of adhesion are unavoidable,[11–13] thus impeding the bonding and coating of WPCs. These adhesion problems to low surface free energy substrates are most often compensated by applying pretreatments that are able to improve the wetting behavior—which, together with the surface roughness, is the most important factor influencing the coating adhesion of WPC, since it increases the surface free energy of the substrate.[14,15]

Gramlich *et al.*[11] demonstrated that chromic acid treatment, flame treatment, water treatment, and sanding can significantly enhance the adhesion characteristics of WPCs. Matuana[16] reported increased surface energy and improved adhesion after fluorooxidation of WPC–substrates. The application of plasmas

Table I. Formulations for PP- and HDPE-Based Wood–Polymer Composites and Processing Conditions

WPC formulations			Processing conditions			
Wood species wt %	Polyolefin wt %	Coupling agent wt %	Processing	Screw(s) rpm	Barrel temperatures °C	Cavity temperature °C
Spruce (60)	PP (40)	MAPP (3)	EX	26	170-185	90
Spruce (60)[a]	PP (40)	MAPP (3)	IM	30	185;185;190;210	90
Spruce (40)[a]	PP (60)	MAPP (3)	IM	30	185;185;185;210	90
Spruce (60)[a]	PP (40)	MAPP (0)	IM	30	185;185;185;210	90
Spruce (60)[b]	HDPE (40)	-	IM	30	185;190:195;200	70

[a] Injection pressure: 60–75 MPa.
[b] Injection pressure: 78–85 MPa.

is a widely used approach to improve adhesion on various hydrophobic surfaces.[17] Akhtarkhavari *et al.*[10] and Gupta and Laborie[18] found increased adhesion of paints and adhesives on WPC after treatment with corona discharge and low-pressure oxygen plasma, respectively.

Wolkenhauer *et al.*[13] showed an increased polar component of the surface free energy and increased surface roughness along with increased bond strength of waterborne and solvent-borne coatings and adhesives for PE- and PP-based WPCs after a dielectric barrier discharge (DBD) treatment at atmospheric pressure. Liu *et al.*[1] detected the generation of polar groups (hydroxyl, carbonyl and carboxyl) on WPC surfaces during air plasma treatment by XPS and Fourier transform infrared spectroscopy (FTIR), improving the wettability and adhesion properties. Similar findings were reported by Hämäläinen *et al.*[19]

The objective of the present study was to compare three different types of air-driven dielectric barrier plasma discharges operated at atmospheric pressure and their effect on the surface properties of various WPC formulations with the focus on changes in surface composition and the improvement in surface wettability and adhesion of the composite. Therefore, several tests and analyses were conducted. The wetting behavior was determined by contact angle measurement and the calculation of surface free energy and the changes in chemical composition (*O*/*C* ratio) were verified by X-ray photoelectron spectroscopy (XPS). Furthermore, the coating performance was evaluated by the crosscut test and the pulloff test.

EXPERIMENTAL

Manufacturing of WPC

The WPC were manufactured by means of two main processing methods, extrusion (EX), and injection molding (IM). In total five formulations were produced, containing spruce (*Picea abies L.*) (Arbocel® C 100; J. Rettenmaier & Söhne GmbH und Co. KG, Rosenberg, Germany), either polypropylene (PP) (SABIC® 575 P, Riyadh, Saudi Arabia) or high density polyethylene (HDPE) (SABIC® HDPE 0863 F, Riyadh, Saudi Arabia), and a coupling agent in three of the five formulations (Licocene® PP MA 6452 Fine grain TP, Clariant International, Muttenz, Switzerland) (Table I).

Profiles were produced in direct extrusion using a parallel twin-screw extruder (MICRO 27 GL/GG 40 D, Leistritz Extrusionstechnik GmbH, Nuremberg, Germany), equipped with a die producing profiles with dimensions of 50 × 4 mm^2. The basic raw materials (wood, polymer, and coupling agent) were put into the heated barrels to melt the polymer. They were then conveyed by the screws and forced into a die to produce the profiles. The material which was processed by injection molding was dry blended first in the same way in the extruder but was then conveyed to a granulator. After that, the granules were fed into the injection molding machine (Arburg Allrounder 420 C Golden, Loßburg, Germany). The cycle time in injection molding was about 52 s, the dosing time 25 s, and the injection time four seconds for all formulations.

For the following tests, the material was cut to a length of 50 mm for the contact angle measurements and XPS analysis, and to a length of 120.5 mm for coating and adhesion tests. Sufficient material was prepared to provide 30 replicates for each WPC formulation and was stored at 20 °C and 65% relative humidity in a climate chamber before the different treatments and tests were conducted.

Plasma Treatment and Setup

The plasma source consists of two bronze electrodes covered with an Al_2O_3 ceramic of 2.5 mm thickness as dielectric material. The electrodes are cooled inside by an air stream. The discharges were all based on the principle of the dielectric barrier discharge (DBD) at atmospheric pressure and driven

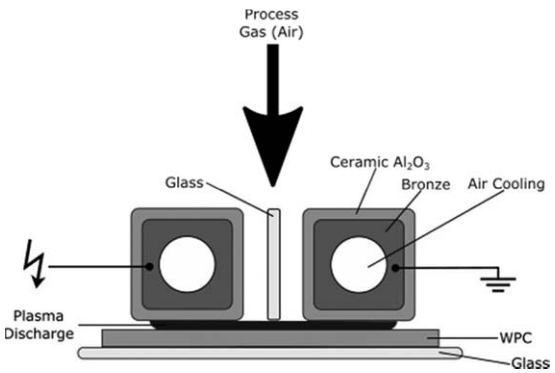

Figure 1. Coplanar surface barrier discharge (CSBD).

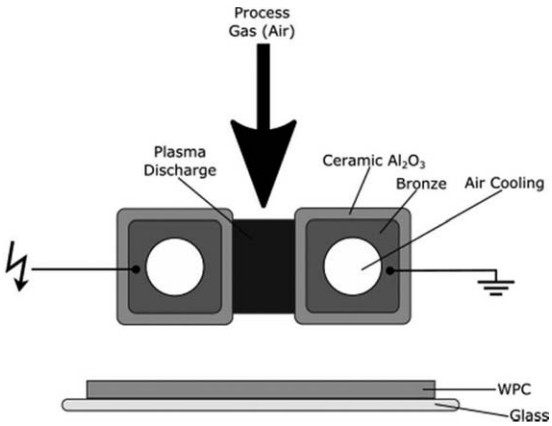

Figure 2. Remote plasma (RP).

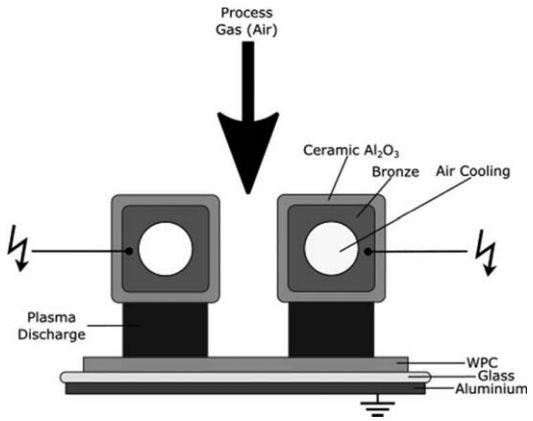

Figure 3. Direct dielectric barrier discharge (DDBD).

with the same basic setup (with small changes) as shown in Figures 1–3.

All three discharges are streamed discharges with ambient air as process gas and a gas volume flow rate of 120 L/min.

For the coplanar surface barrier discharge (CSBD),[20,21] both electrodes are separated by a distance of 15 mm, with a 3 mm float glass as an additional dielectric material between them and a distance to the sample surface of about 0.5 mm. The first electrode is connected to the high voltage power supply while the second is grounded (Figure 1).

For the remote plasma discharge (RP) as well as for the direct dielectric barrier discharge (DDBD), the electrodes are separated by a distance of 2 mm as well as a distance of 2 mm to the sample surface; the additional glass between the electrodes is removed. Their difference is the electrical connection (Figures 2 and 3). For the remote plasma discharge,[22] the connection is the same as for the CSBD.

For the direct dielectric barrier discharge, as shown in Figure 3, both electrodes are connected to the high voltage power supply. Here, the aluminum plate covered by glass constitutes the grounded electrode.

Each second of plasma treatment was followed by a pause of the same time (1 s) for lowering the thermal impact on the surface. The net plasma treatment duration was 10 s. The high voltage power supply provides alternating pulses with a pulse repetition frequency of 15 kHz. The plasma parameters are listed in Table II.

To determine the power which was injected into the plasma, the applied voltage was measured by a high voltage probe PVM-1 from HVP High Voltage Products GmbH, Martinsried/Planegg, Germany, and the transferred charge by the voltage curve on a capacitance (WIMA, FKP1.2× 100 nF).[23–27]

Surface Analysis

Contact Angle Measurement and Calculation of Surface Free Energy. The contact angle measurement of untreated and plasma-treated specimens was carried out using the device G 10, Krüss GmbH, Hamburg, Germany, and the static sessile drop method using four probe liquids (distilled water, diiodomethane, ethylene glycol, and glycerol). The dosing parameters were: drop size of 10 µL and a rate of 450 µL/min for water, 7 µL and 1500 µL/min for diiodomethane, 20 and 1500 µL/min for ethylene glycol, and 40 µL and 1500 µL/min for glycerol. The surface tensions according to Ström *et al.*[28] were applied to calculate the surface free energy.

After depositing the drop, a picture was taken. On the basis of this picture, the software DSA 1 v 1.90 (Krüss GmbH, Hamburg, Germany), was used to determine the contact angle by the conic section method, which describes the drop shape as an elliptical arc on the surface.

For each variant, three samples were tested and four droplets of each liquid were deposited on the surface of each sample. Thus, the average and the corresponding standard deviation of twelve measurements for each liquid and variant were reported. The contact angle measurement was completed within ten minutes after plasma treatment to avoid aging processes.[29]

Based on the contact angles, the surface free energy was calculated according to the geometric mean approach of Owens and Wendt, which allows the total surface free energy (σ_s) to be resolved into a polar part (σ_s^P) and a dispersive (σ_s^D) or nonpolar part[30]:

Table II. Parameters of the Three Discharge Types

	CSBD	RP	DDBD
Power	178 ± 9 W	163 ± 0.5 W	153 ± 0.3 W
Max. voltage amplitude	28.8 ± 0.1 kV	19.8 ± 0.1 kV	24.2 ± 0.1 kV

Table III. Water Contact Angles and the Standard Deviation of the Untreated References and after Plasma Activation by Three Discharge Types (CSBD, DDBD, and RP)

WPC formulations				Manufacturing	Distilled water	
Type of discharge	Wood species wt %	Polyolefin wt %	Coupling agent (%)[a]	Processing method	Contact angle Deg	Standard deviation Deg
Reference	Spruce (60)	PP (40)	MAPP (3)	EX	98.5	1.2
CSBD					59.9	0.6
DDBD					63.2	3.9
RP					68.1	3.1
Reference	Spruce (60)	PP (40)	MAPP (3)	IM	98.9	1.6
CSBD					61.4	3.1
DDBD					68.8	2.1
RP					66.8	4.0
Reference	Spruce (40)	PP (60)	MAPP (3)	IM	92.4	5.9
CSBD					59.0	1.7
DDBD					62.0	8.7
RP					66.8	1.6
Reference	Spruce (60)	PP (40)	MAPP (0)	IM	93.6	2.0
CSBD					68.5	3.1
DDBD					67.7	2.8
RP					67.6	1.3
Reference	Spruce (60)	HDPE (40)	-	IM	88.8	8.8
CSBD					60.6	6.8
DDBD					48.5	12.8
RP					57.1	1.9

[a]MAPP: maleic anhydride grafted polypropylene.

$$\sigma_s = \sigma_s^P + \sigma_s^D \quad (1)$$

The interfacial tension between a solid and a liquid is evaluated by the geometric mean equation:

$$\sigma_{sl} = \sigma_s + \sigma_l - 2\sqrt{\sigma_s^D \sigma_l^D} + \sqrt{\sigma_s^P \sigma_l^P} \quad (2)$$

with the dispersive (σ_l^D) and polar (σ_l^P) parts of the liquid, and the dispersive (σ_s^D) and polar (σ_s^P) parts of the solid. Young's equation,[31] which expresses the balance on the three-phase interface, has to be mentioned:

$$\sigma_s = \sigma_{sl} + \sigma_l * \cos\theta \quad (3)$$

where σ_s is the total surface energy of a solid in mN/m, σ_{sl} is the interfacial tension between solid and liquid, σ_l is the surface tension of the test liquid, and θ is the contact angle. Based on the assumption that the surface tension is composed of two components, they establish the following geometric mean equation:

$$\frac{(1+\cos\theta)\cdot\sigma_l}{2\sqrt{\sigma_l^D}} = \sqrt{\sigma_s^P}\sqrt{\frac{\sigma_l^P}{\sigma_l^D}} + \sqrt{\sigma_s^D} \quad (4)$$

For determining the surface energy parts ($\sigma_s^P$and σ_s^D), the left term (eq. 4) is plotted as a function of the polar and dispersive parts of the liquid surface tension. The polar surface tension part is calculated by the gradient of the linear regression and the dispersive part by the y axis intercept.

XPS Measurement. XPS analysis was performed using a PHI 5000 Versa Probe II spectrometer (Physical Electronics, Ismaning, Germany) equipped with a 180° spherical energy analyzer and a multichannel detection system. Spectra were acquired at a base pressure of 5×10^{-7} Pa using a monochromatic Al-Kα source (1486.6 eV) with a spot diameter of 200 µm.

The data were analyzed using the program MultiPak (V 9.4.0.7, 2012-11-27). Atomic concentrations were calculated for C1s and O1s peaks using a Shirley background;[32] the corresponding cross-sections were automatically included in the calculation by MultiPak and were in accordance with cross-sections provided by Yeh and Lindau.[33] Survey spectra were recorded using pass energy of 188 eV and a step size of 0.8 eV. To make sure the surfaces of the samples were free of any contaminants, they were cleaned with isopropyl alcohol before conducting the XPS analysis.

Coating Adhesion of WPC. The samples were coated within one hour after plasma treatment using an acrylic paint. Two layers of paint were applied manually with a roller about 5.3 cm wide (adapted for the sample geometry). Before application, surplus paint was removed by stripping off the roller in a paint tray. Information on the coating uptake was gained by checking the mass change before and after applying the first layer. After a drying time of 24 h at room temperature, the next layer was applied, and the tests were conducted. In total, four

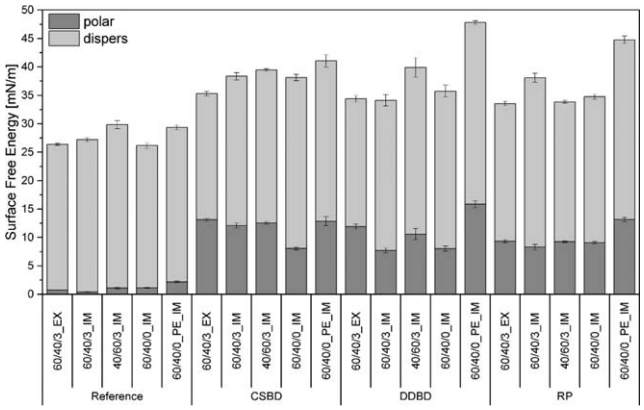

Figure 4. Surface free energy data of various WPC formulations before and after plasma treatment by different discharge types; split into polar part and dispersive part; bars: mean values; error bars: standard error ($N = 12$ for each formulation).

replicates for each formulation and each discharge type were prepared in this way.

The adhesion properties before and after plasma surface activation of the coated samples were evaluated with two tests: the crosscut test according to the German standard DIN EN ISO 2409[34] and the pulloff test according to the German standard DIN EN ISO 4624.[35] In addition to these standardized methods, an image analysis was conducted to estimate the area of paint delamination caused by the adhesive tape used in the crosscut test. For this purpose, the samples were scanned in black-and-white mode. Afterwards, the captured images were processed in MATLAB R2013b to detect the detached area. The number of pixels, painted or detached, were thereby counted and set into relation to each other to calculate the percentage of delamination.

RESULTS AND DISCUSSION

Surface Analysis

The results revealed that the water contact angle measurements (shown in Table III) decreased after each of the three applied plasma treatments. The reference showed values between 88° and 98°, while the average static contact angles of the treated samples ranged between 48° and 68°. It became obvious that the lowest contact angles were achieved for the PE-based WPC—both for the reference and for the treated surfaces. Differences in wetting behavior within the plasma-activated samples were not evident.

The water contact angle decreased as a result of the plasma treatment, which is known to improve the wetting behavior of low surface energy substrates, such as WPCs, as stated by several studies.[1,19,36] The values for the contact angles measured on the PP references at about 90°–98° approximately correspond to those for neat polypropylene.[37,38] The PE-based WPCs showed the lowest contact angles before and after plasma treatment. This might be due to the slightly higher initial surface energy of PE compared to PP as it is reported by Yao *et al.*[39]

The decrease in contact angle corresponds to an increase in surface free energy. In particular, the polar part is affected by the plasma treatment (Figure 4). By applying the DDBD discharge, the highest values for the total surface free energy could be generated with the PE-based WPC (more than 45 mN/m). The PE-based composites showed slightly higher values than the other formulations. Similar results could be observed for the combination of RP and 60/40/0_PE_IM.

As mentioned, the polar part showed a distinct change after the plasma treatment, independent on the type of discharge. These findings could be explained by the generation of functional groups, such as —OH, —C═O and —O—C═O—a process which is initiated by an oxidation of the surface.[1,40] The highest surface free energy before and after plasma treatment could be achieved for the PE-based WPCs. These results correspond to the higher initial surface energy, which could be evaluated by the contact angle data as well.

Oxygen/Carbon Ratio. In addition, changes in the elemental composition of the surface were experimentally verified by XPS analysis. Figure 5 shows exemplary survey spectra of untreated and CSBD-treated PE-based WPC (60/40/0_IM_PE). As can be seen, the plasma treatment led to a significant increase of the oxygen peak.

The *O*/*C* ratio, therefore, increased in comparison to the references, from about 0.025 to 0.2 (Figure 6). Moreover, it was apparent that the CSBD discharge caused the PE-based WPC formulation to reach the maximum in *O*/*C* ratio which was 0.2. In addition, it could be stated that treating the formulation with lower wood content (40/60/3_IM) led to more homogenous results for the *O*/*C* ratio with fewer differences when comparing the three discharge types among themselves. The remote plasma showed the highest *O*/*C* ratio for the material 60/40/3_EX, while for DDBD and CSBD the biggest change was visible for 60/40/0_IM and 60/40/0_IM_PE.

A proof for the changes in the chemical composition of the surface (i.e., a shift in carbon and oxygen content) can be given by the XPS analysis shown by the results. The *O*/*C* ratio increased after plasma treatment, which is indicative for an oxidation by

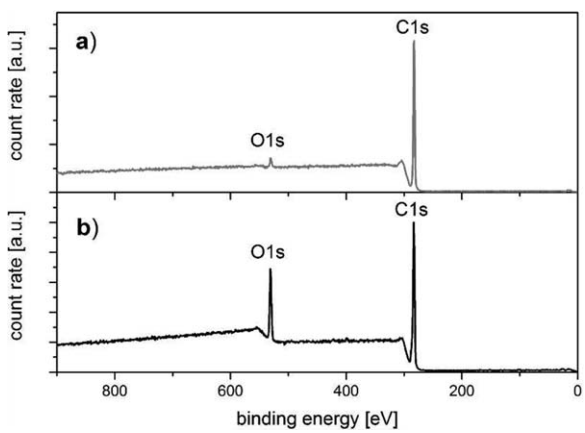

Figure 5. Survey spectra of untreated (a) and CSBD-treated (b) PE-based WPC.

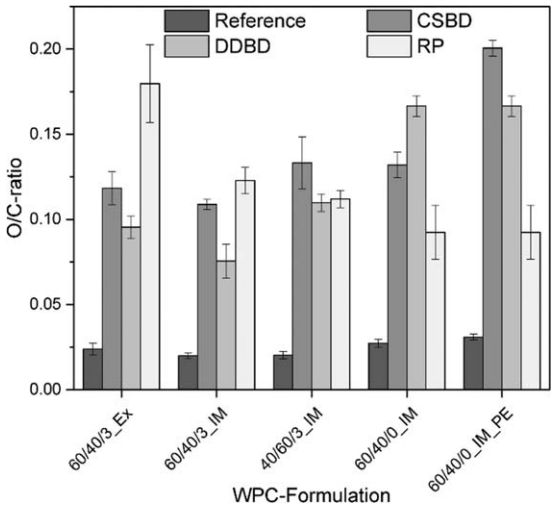

Figure 6. O/*C* ratio of the untreated and plasma-treated surfaces; bars: mean values; error bars: standard error ($N = 20$ for each formulation).

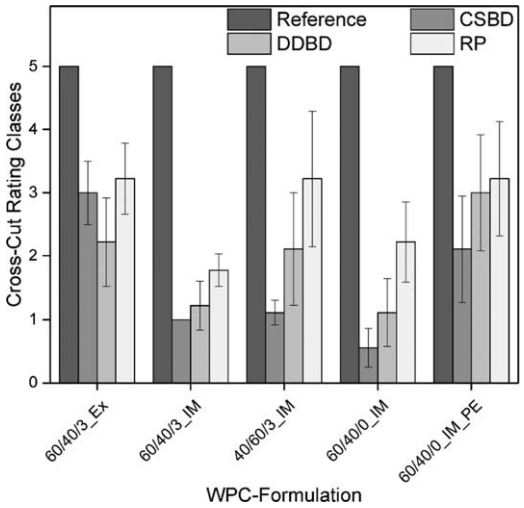

Figure 8. Crosscut test according to DIN EN ISO 2409; bars: mean values; error bars: standard error ($N = 10$ for each formulation).

the electrical discharge similar to results observed in polyolefins.[41] In addition, it can be assumed that the more homogenous results in the *O*/*C* ratio which were gained for the formulation 40/60/3_IM are due to the lower wood content in the composite and at the surface, leading to a smoother surface finish.[15] As a consequence, the outer layers of the substrate might be more chemically homogenous and thus the plasma oxidation might lead to a more even distribution.

Coating

The pretreatment of the substrate surface had a positive effect on the coating uptake (Figure 7). Although two layers were applied to the material, the data presented in this paper relate to the base layer, because it is here that the adhesion between the plasma-treated substrate surface and the coating takes place. An increase in coating uptake was observed for all five variants. This increase is caused by the improvement in wettability due to the generation of functional groups (mentioned above) and probably by an increase in surface roughness, which is also responsible for good adhesion properties.[13,42] The average application quantity ranged from 93 g/m^2 for the references to 121 g/m^2 for the material which was pretreated by the direct dielectric barrier discharge. The other four variants showed results of 57 g/m^2 for the references and about 86 g/m^2 after plasma treatment. The highest uptake (123 g/m^2) was measured for the material 60/40/3_EX. Even the references which had not been pretreated showed higher uptakes than all other treated materials. This indicates that the adhesion of this untreated extruded material shows a better initial coatability than the formulations that are compared with it. These findings were in accordance with the literature. Stark *et al.*[43] reported that injection-molded sample surfaces were polymer-rich and thus of poor polarity, whereas the wood particle content at the surface in extruded WPC is more apparent. Moreover, Stark[44] observed an incomplete encapsulation of wood particles by the polymer, which was proved for injection molded material. Another finding was a lower standard error in mass change for the activated surfaces compared to the references. On the basis of these results, it became obvious once again that a homogenization in surface finish had taken place. This means that the paint could be more evenly distributed on the single samples.

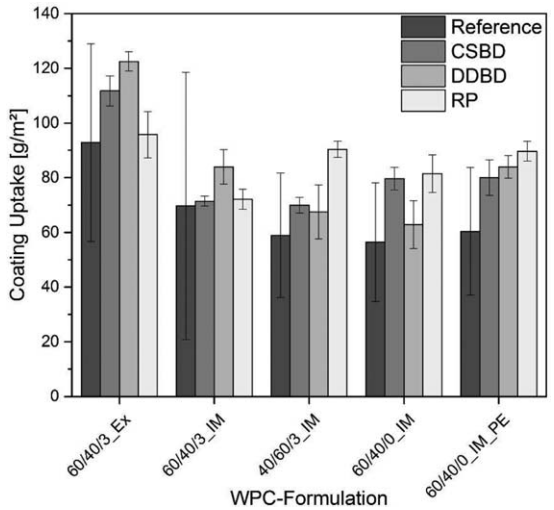

Figure 7. Influence of plasma treatment on coating uptake; bars: mean values; error bars: standard error ($N = 10$ for each formulation).

Adhesion Tests

The adhesive strength was evaluated by the standardized crosscut test according to the standard DIN EN ISO 2409[34] (Figure 8). The poor adhesion of the references could be expressed by class five, whereas the activated surfaces with plasma reached at least class three. The highest adhesive strength was reached after a pretreatment by the discharge types CSBD and DDBD with values between one and three. The remote plasma has, in contrast to the CSBD and DDBD discharges, no direct contact to the surface. Based on the principle of the RP, the plasma generation occurs at a distance of about 2 mm above the surface to be treated and accrued radicals are

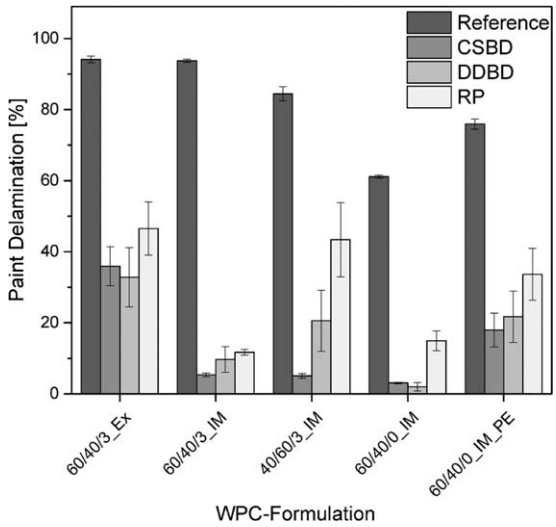

Figure 9. Paint delamination after crosscut test before and after plasma pretreatment; bars: mean values; error bars: standard error ($N = 10$ for each formulation).

transported indirectly to the outer substrate layer by an air stream. Therefore, the reason for the weaker adhesion improvement for the remote plasma-treated samples might be attributed to the fact that surfaces are merely exposed to plasma-generated species which show relatively extended lifetimes or were generated during afterglow (e.g., O_3) and are less reactive compared to species exhibiting short lifetimes (e.g., O).[45]

Furthermore, a certain influence of discharge filaments to substrate surface—resulting in altered surface roughness (as shown by Wolkenhauer *et al.*[13] for a direct DBD)—can be expected for the direct treatment methods CSBD and DDBD and might contribute to adhesion improvement.

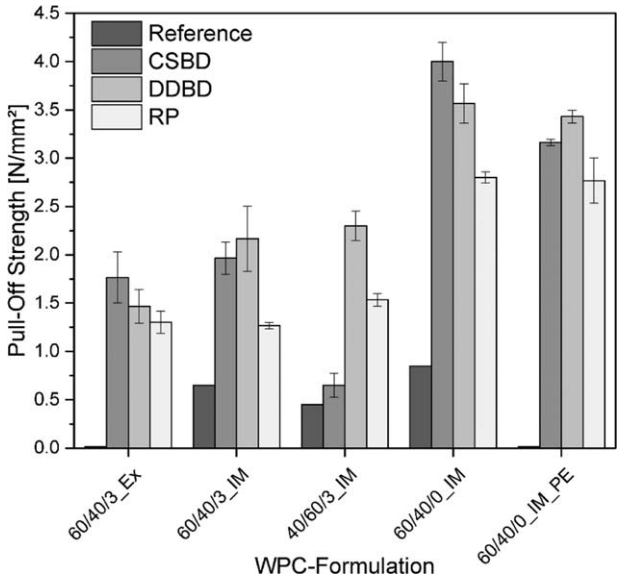

Figure 10. Pulloff test according to DIN EN ISO 4624 before and after plasma treatment; bars: mean values; error bars: standard error ($N = 10$ for each formulation).

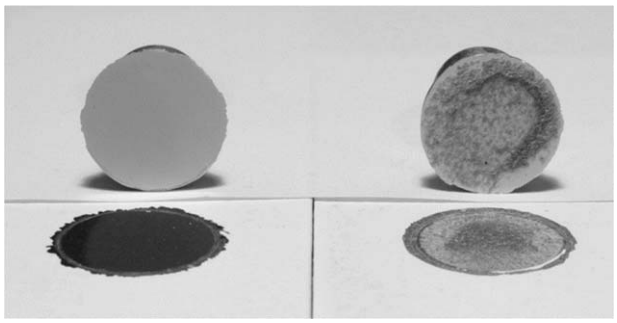

Figure 11. Pulloff test; samples with (left) and without (right) coupling agent.

The explanation above can be used to interpret all adhesion tests conducted in this study.

As a complementary evaluation to the standardized crosscut test, a visual analysis of the inspected area of the crosscut was done to estimate the amount of paint detached by the adhesive tape. The corresponding results are shown in Figure 9. According to the results gained from the crosscut test, a diminished paint delamination after pretreatment of the coated surfaces could be observed. Here again, the two discharge types CSBD and DDBD proved to be the most effective. While the delaminated area for the references was between 60 and 100% of the testing area, the average area in the case of plasma-treated surfaces for the discharge types CSBD and DDBD was less than 40% and for the remote plasma below 60% for all tested formulations. Minimal paint delamination (i.e. less than 10%) was observed for the CSBD discharge for the formulations WPC_60_40_3_IM, WPC_40603_IM and WPC_60400_IM. The DDBD-treated material showed similar results for the variants 60_40_3_IM and WPC_60400_IM. Again, the poorer adhesion gained by RP became obvious.

The observed results were in accordance with those reported by Wolkenhauer *et al.*[13] and Gupta, Reiniati and Laborie.[46]

Figure 10 shows the results of the pulloff test for adhesion that was done according to the standard DIN EN ISO 4624.[35] The purpose of this standardized testing method was to determine the pulloff strength of a coating from a solid substrate.

Also these results showed a distinct increase in adhesion of the substrate. Whilst the references gained values of about 0.5 N/mm^2, the pretreated material was at least 1 N/mm^2. Moreover, it is remarkable that the two formulations without coupling agent (60/40/0_IM and 60/40/0_PE_IM) showed higher values (2.5–4 N/mm^2) after pretreatment. The references for the two formulations 60/40/3_Ex and 60/40/0_IM_PE could not be measured on account of their poor adhesion because, due to this, sample preparation was not possible according to the standard.

The results of the pulloff test have to be evaluated differently. The values gained from the formulations without coupling agents (60/40/0_IM and 60/40/0_IM_PE) showed a cohesive rather than an adhesive failure near the surface (Figure 11).

Based on these findings it can be concluded that the cohesion within the bulk material was weaker than the adhesion between the two phases created by the coating and the WPC surface. The reason for this is the weaker binding between the hydrophilic wood and the hydrophobic polymer.[47] Adding a coupling agent leads to higher strength of the composite.[48]

CONCLUSIONS

Five formulations of WPCs were treated with atmospheric-pressure plasma to improve their adhesion with an acrylic coating. One aim was to compare the efficacy of various types of discharges that were used for activating the WPC surfaces. Another was to evaluate the interaction between the discharges and the different formulations of WPC. The *O*/*C* ratio, wettability, and coating adhesion were determined by XPS, contact angle measurements, and adhesion tests. In general it can be concluded that the surface pretreatments led to a distinct increase in surface wettability, independent of the WPC formulation and discharge type. For the PE-based WPC, the polar content showed the highest increase compared to the other formulations. The extruded material also showed slightly higher values than the injection-molded composites. Moreover, the effect of the plasma treatment could be noted by an increase in oxygen content in XPS, which was observed in all formulations. A homogenization of the surface quality was exemplified by lower variation of the collected data for the treated material. The results for the coating adhesion tests showed better values for the material treated with DDBD and CSBD. It is noteworthy that the RP-treatment improved wettability to a similar extent and resulted also in a high *O*/*C* ratio, but poorer adhesion was observed in the coating tests. Thus, for further treatments related to coating adhesion, it is suggested that either DDBD or CSBD be used to activate WPC surfaces. Nevertheless, RP might also have fields of application due to its flexible treatment properties on the surfaces. The best adhesion could be seen for the extruded material and the PE-based WPC formulation.

ACKNOWLEDGMENTS

This work was funded by the German Federal Ministry of Education and Research (BMBF), under the supervision of Dr.-Ing. Karen Otten, in Jülich, Germany, and the joint research project "PlaNaWood" (Grant No. 03X5519A).

REFERENCES

1. Liu, Y.; Tao, Y.; Lv, X.; Zhang, Y.; Di, M. *Appl. Surf. Sci.* **2010**, *257*, 1112.
2. Gardner, D.; Han, Y.; Wang, L. *Curr. For. Rep.* **2015**, *1*, 139.
3. Carus, M.; Eder, A.; Dammer, L.; Korte, H.; Scholz, L.; Essel, R.; Breitmayer, E. Available at: http://bio-based.eu/download/?did=18787=file=0. Accessed on 5 August 2015.
4. Fabiyi, J. S.; McDonald, A. G.; Wolcott, M. P.; Griffiths, P. R. *Polym. Degrad. Stabil.* **2008**, *93*, 1405.
5. Butylina, S.; Hyvarinen, M.; Karki, T. *Polym. Degrad. Stabil.* **2012**, *97*, 337.
6. Stark, N. M.; Matuana, L. M. *J. Appl. Polym. Sci.* **2003**, *90*, 2609.
7. Ndiaye, D.; Fanton, E.; Morlat-Therias, S.; Vidal, L.; Tidjani, A.; Gardette, J. L. *Compos. Sci. Technol.* **2008**, *68*, 2779.
8. Hon, D. N.-S. In Wood and Cellulose Chemistry; Hon, D. N.-S.; Shiraishi, N., Eds.; Marcel Dekker, Inc.: New York, **2001**; p 513.
9. Brostow, W.; Datashvili, T.; Miller, H. *J. Mater. Educ.* **2010**, *32*, 125.
10. Akhtarkhavari, A.; Kortschot, M. T.; Spelt, J. K. *Prog. Org. Coat.* **2004**, *49*, 33.
11. Gramlich, W. M.; Gardner, D. J.; Neivandt, D. J. *J. Adhes. Sci. Technol.* **2006**, *20*, 1873.
12. Novák, I.; Pollák, V.; Chodák, I. *Plasma Process Polym.* **2006**, *3*, 355.
13. Wolkenhauer, A.; Avramidis, G.; Hauswald, E.; Militz, H.; Viol, W. *J. Adhes. Sci. Technol.* **2008**, *22*, 2025.
14. Ryntz, R. A. *Prog. Org. Coat.* **1994**, *25*, 73.
15. Ayrilmis, N.; Benthien, J. T.; Thoemen, H. *Compos. B: Eng.* **2012**, *43*, 325.
16. Matuana, L. M. *J. Vinyl Addit. Technol.* **2009**, *15*, 136.
17. Hippler, R. Low Temperature Plasma Physics: Fundamental Aspects and Applications; Wiley-VCH: Berlin, **2001**.
18. Gupta, B. S.; Laborie, M. P. G. *J. Adhes.* **2007**, *83*, 939.
19. Hämäläinen, K.; Kärki, T. *Adv. Mater. Res.* **2013**, *718720*, 176.
20. Lux, C.; Szalay, Z.; Beikircher, W.; Kováčik, D.; Pulker, H. *Eur. J. Wood Prod.* **2013**, *71*, 539.
21. Odrášková, M.; Ráheľ, J.; Zahoranová, A.; Tiňo, R.; Černák, M. *Plasma Chem. Plasma Process.* **2008**, *28*, 203.
22. Gonzalez, E.; Barankin, M. D.; Guschl, P. C.; Hicks, R. F. *Langmuir* **2008**, *24*, 12636.
23. Kogelschatz, U. *Plasma Chem. Plasma Protein* **2003**, *23*, 1.
24. Wascher, R.; Avramidis, G.; Vetter, U.; Damm, R.; Peters, F.; Militz, H.; Viöl, W. *Surf. Coat. Technol. A* **2014**, *259*, 62.
25. Helmke, A.; Hoffmeister, D.; Mertens, N.; Emmert, S.; Schuette, J.; Vioel, W. *New J. Phys.* **2009**, *11*, 115025.
26. Falkenstein, Z.; Coogan, J. *J. Phys. D: Appl. Phys.* **1997**, *30*, 817.
27. Manley, T. C. *Trans. Electrochem. Soc.* **1943**, *84*, 83.
28. Ström, G.; Fredriksson, M.; Stenius, P. *J. Colloid Interface Sci.* **1987**, *119*, 352.
29. Garbassi, F.; Morra, M.; Occhiello, E.; Barino, L.; Scordamaglia, R. *Surf. Interface Anal.* **1989**, *14*, 585.
30. Owens, D. K.; Wendt, R. C. *J. Appl. Polym. Sci.* **1969**, *13*, 1741.
31. Young, T. *Philos. Trans. Roy. Soc. Lond.* **1805**, *95*, 65.
32. Shirley, D. A. *Phys. Rev. B.* **1972**, *55*, 4709.
33. Yeh, J. J.; Lindau, I. *Atomic Data Nucl. Data Tables* **1985**, *32*, 1.
34. DIN EN ISO 2409. Beuth Verlag GmbH: **2007**−08.
35. DIN EN ISO 4624. Beuth Verlag GmbH: **2003**−08.
36. Nishime, T. M. C.; Toth, A.; Hein, L. R. O.; Kostov, K. G. *J. Phys. Conf. Ser.* **2012**, *370*,
37. Morra, M.; Occhiello, E.; Gila, L.; Garbassi, F. *J. Adhes.* **1990**, *33*, 77.

38. Sutherland, I.; Brewis, D. M.; Heath, R. J.; Sheng, E. *Surf. Interface Anal.* **1991**, *17*, 507.
39. Yao, Y.; Liu, X.; Zhu, Y. *J. Adhes. Sci. Technol.* **1993**, *7*, 63.
40. Tao, Y.; Di, M. W. *Appl. Mech. Mater.* **2011**, *6668*, 911.
41. Liston, E. M.; Martinu, L.; Wertheimer, M. R. *J. Adhes. Sci. Technol.* **1993**, *7*, 1091.
42. Hutyrova, Z.; Harnicarova, M.; Zajac, J.; Valicek, J.; Mihok, J. *Adv. Mater. Res.* **2014**, *856*, 108.
43. Stark, N. M.; Matuana, L. M.; Clemons, C. M. *J. Appl. Polym. Sci.* **2004**, *93*, 1021.
44. Stark, N. M. *J. Appl. Polym. Sci.* **2006**, *100*, 3131.
45. Wende, K.; Williams, P.; Dalluge, J.; Van Gaens, W.; Aboubakr, H.; Bischof, J.; von Woedtke, T.; Goyal, S. M.; Weltmann, K. D.; Bogaerts, A.; Masur, K.; Bruggeman, P. J. *Biointerphases* **2015**, *10*, 029518.
46. Gupta, B. S.; Reiniati, I.; Laborie, M. P. G. *Colloids Surf. A: Physicochem. Eng. Aspects* **2007**, *302*, 388.
47. Benthien, J. T.; Thoemen, H. *Compos. A: Appl. Sci.* **2012**, *43*, 570.
48. Ayrilmis, N.; Jarusombuti, S. *J. Compos. Mater.* **2010**, *0*, 1.